Image Cover Sheet

CLASSIFICATION	SYSTEM NUMBER
UNCLASSIFIED	127315

TITLE

TESTING VARIOUS TIME-FREQUENCY DISTRIBUTION TECHNIQUES

System Number:

Patron Number:

Requester:

Notes:

DSIS Use only:

Deliver to: JR

National Defence / Défense nationale

TESTING VARIOUS TIME-FREQUENCY DISTRIBUTION TECHNIQUES (U)

by

Robert Klepko and Khanh N. Tran

DEFENCE RESEARCH ESTABLISHMENT OTTAWA
TECHNICAL NOTE 92-17

Canada

November 1992
Ottawa

National Defence / Défense nationale

TESTING VARIOUS TIME-FREQUENCY DISTRIBUTION TECHNIQUES (U)

by

Robert Klepko
Airborne Radar Section
Radar Division

and

Khanh N. Tran
Co-op Student, Computer Engineering
University of Ottawa (ID 573328)

DEFENCE RESEARCH ESTABLISHMENT OTTAWA
TECHNICAL NOTE 92-17

PCN
021LA

November 1992
Ottawa

ABSTRACT

The representation of a signal in both the time and frequency domains is a major topic of study in the area of signal processing. Over the past 40 years, many plausible derivations and approaches of time-frequency distributions have been suggested. This paper tests two time-frequency distributions and compares their results. The two distributions are the discrete versions of the Wigner-Ville and Choi-Williams distributions. This paper will demonstrate the capability of each distribution to resolve discrete sinusoidal and real radar signals simultaneously in time and frequency. The radar data represents backscatter from a ship on the open ocean. The results will be presented in both a graph and table format. These results will be compared to those obtained from the standard short-time Discrete Fourier Transform.

RÉSUMÉ

La représentation simultanée d'un signal dans les domaines du temps et des fréquences est un sujet d'étude important en analyse de signaux. Au cours des 40 dernières années, de nombreuses dérivations de distributions ont été suggérées. Ce document évalue deux distributions dans le domaine temps-fréquence et compare les résultats. Les deux distributions sont les versions discrètes des distributions de Wigner-Ville et Choi-Williams. Ce rapport démontrera les limites de résolution de chacune des distributions pour des signaux discrets sinusoidaux et des signaux radars réels. Les données radars sont des signatures de bateaux prises en haute mer. Les résultats seront présentés à l'aide de graphiques et de tables. Ils seront comparés à ceux obtenus à l'aide de la méthode standard de la Transformée de Fourier.

EXECUTIVE SUMMARY

The representation of a signal in both the time and frequency domains is a topic of great interest in the area of digital signal processing. The desired goal is to devise a distribution that simultaneously represents the energy or intensity of a signal in both time and frequency. Time-Frequency Distributions (TFDs) are best applied to non-stationary signals. This important class of signals is commonly found in the real world. Typical application areas include radar, sonar and seismology.

Over the past 40 years, many plausible derivations and approaches of TFDs have been suggested. Considerable differences in the behaviour of the various distributions were observed. In this paper, the Choi-Williams and Wigner-Ville distributions will be examined. These are the two most popular forms of TFDs. Only the discrete versions of these TFDs will be tested. The results associated with the two distributions will also be compared to those obtained with the standard short-time Discrete Fourier Transform (DFT).

The tests will be performed with discrete simulated sinusoidal signals as well as with real signals. The real signals considered represent the temporal radar backscatter collected from a Synthetic Aperture Radar (SAR). The general properties of the backscatter are the fading in and out of narrowband signals and shifting of signal frequency through time as a result of scatterer motion. Using a TFD allows an analysis of the Doppler frequency history of the scatterers located on a target of interest (e.g. a ship moving on the open ocean).

The major conclusion to be drawn from the tests performed with real signals is that the Choi-Williams distribution is preferred over both the Wigner-Ville distribution and DFT as a result of improved Signal-to-Noise Ratios in the spectral domain.

The eventual goal of this study is to determine whether the conventional use of the DFT within the signal processing domain of a radar system should be replaced by a TFD technique. TFDs may allow better tracking, detection and resolvability of signals.

TABLE OF CONTENTS

LIST OF FIGURES

LIST OF TABLES

1. INTRODUCTION

The representation of a signal in both the time and frequency domains is a topic of great interest in the area of digital signal processing. The desired goal is to devise a distribution that simultaneously represents the energy or intensity of a signal in both time and frequency. Time-Frequency Distributions (TFDs) are best applied to non-stationary signals. This important class of signals is commonly found in the real world. Typical application areas include radar, sonar and seismology.

Over the past 40 years, many plausible derivations and approaches of TFDs have been suggested. Considerable differences in the behaviour of the various distributions were observed. In this paper, the Choi-Williams and Wigner-Ville distributions will be examined. These are the two most popular forms of TFDs. Only the discrete versions of these TFDs will be tested. The results associated with the two distributions will also be compared to those obtained with the standard short-time Discrete Fourier Transform (DFT).

The tests will be performed with discrete simulated sinusoidal signals as well as with real signals. The real signals considered represent the temporal radar backscatter collected from a Synthetic Aperture Radar (SAR). The general properties of the backscatter are the fading in and out of narrowband signals and shifting of signal frequency through time as a result of scatterer motion. Using a TFD allows an analysis of the Doppler frequency history of the scatterers located on a target of interest (e.g. a ship moving on the open ocean).

The results of the study are reported in the next three sections. Section 2 describes the two distribution techniques considered, namely the Choi-Williams and Wigner-Ville distributions. Section 3 describes the tests performed and test data used. In addition, a comparison of the test results with those obtained from the short-time DFT is presented. Section 4 summarizes the findings and suggests further investigations.

2. TIME-FREQUENCY DISTRIBUTION METHODS

Two different approaches can be distinguished to compute TFDs. The first is by means of analogue signal processing, and the second is by means of digital signal processing, representing the continuous and discrete time domains, respectively. In this paper, only discrete-time signals will be analyzed. Furthermore, only the TFD methods of Choi-Williams and Wigner-Ville will be examined. The two following subsections will briefly describe each method.

For further theoretical information on TFDs, the interested readers can refer to reference [1].

2.1. The Choi-Williams Method

Choi and Williams [2] succeeded in devising a new technique of time versus frequency distribution which behaves remarkably well. It satisfies our intuitive notions with respect to the locations of the signal energy. It also reduces, to a large extent, the spurious cross-terms characteristic of multicomponent signals. Cross-terms represent unwanted signal energy which results from interactions between pairs of different signal components within the composite signal. These terms do not permit a straightforward interpretation of the energy distribution. The desirable properties of a time-frequency distribution are also satisfied by the Choi-Williams Distribution. These properties are discussed in [1].

The discrete-time form of the CWD is :

$$CWD(n,k) = 2\sum_{\tau=-\infty}^{+\infty} W_N(\tau)e^{-(j2\pi k\tau/N)} \cdot \left[\sum_{\mu=-\infty}^{+\infty} W_M(\mu)\frac{1}{\sqrt{4\pi\tau^2/\sigma}}e^{-\left[\frac{\mu^2}{4\tau^2/\sigma}\right]} \cdot f(n+\mu+\tau)\cdot f^*(n+\mu-\tau)\right], \quad (1)$$

where

σ : is an adjustable amplitude scaling parameter,
μ,τ : are the dummy-variables representing the time domain,
n,k : are the discrete time and frequency indices, respectively,
N,M : are the sizes of the windows
$f(n)$: is the discrete-time form of the input complex signal, and
$f^*(n)$: is the complex conjugate of the discrete-time input signal.

In Equation (1), the term in the square bracket is referred to as the time indexed autocorrelation function.

The Choi-Williams method will be tested with discrete-time input signals. The Fast Fourier Transform (FFT) technique will be used to realize the first summation in Equation (1). This will allow a significant speed up in the computation of this distribution. The flowchart of the algorithm used for the evaluation of this distribution is given in Figure 1 for non-analytic signals (i.e. non-complex signals). Figure 2 gives the flowchart for analytic signals. Analytic signals are complex signals with zero energy in the negative frequency domain (i.e. $-\pi \leq \omega < 0$) [10]. This distribution, as well as the Wigner-Ville Distribution, requires that the input data be analytic in order to bandlimit the input signals so that they are periodic with a period of π instead of 2π. This eliminates aliasing problems with the distribution. The process of making a signal analytic effectively reduces the sampling rate of the signal by a factor of two. This in turn increases, by a factor of two, the frequency resolution of the output spectrum. Note that both distributions are periodic with a period π (i.e. $0 \leq \omega \leq \pi$), but all spectra of discrete-time signals are periodic with a period 2π (i.e. $-\pi \leq \omega \leq \pi$).

A more detailed discussion of the properties and background theory of the CWD is beyond the scope of this paper. The interested reader can refer to the papers by Choi and Williams [2], and Cohen [1].

2.2. The Wigner-Ville Method

The Wigner-Ville Distribution (WVD) was the first distribution proposed and is the most widely studied and used. This distribution is particularly suited for the time-frequency analysis of stationary signals. It played a major role in the development of the field of TFD techniques [1].

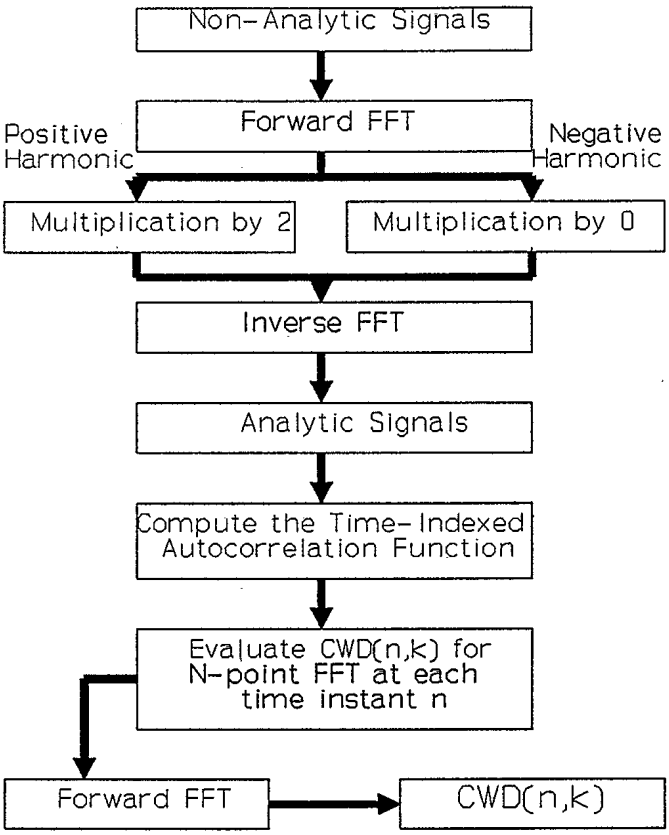

Figure 1. *Flowchart of the algorithm used for the evaluation of the Choi-Williams distribution with non-analytic input signals.*

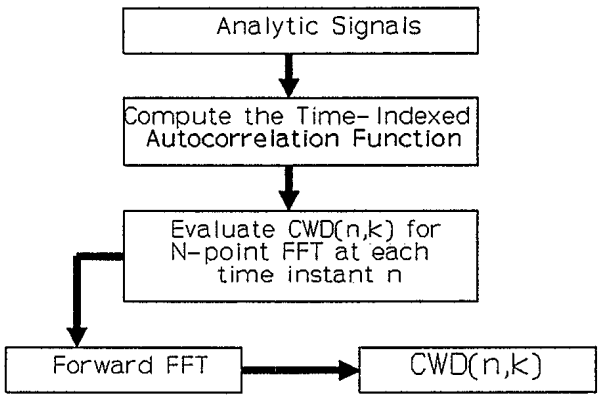

Figure 2. Same as Figure 1, but for analytic input signals.

The Wigner-Ville distribution in the discrete-time domain is defined as :

$$W_{f,g}(n,m\frac{\pi}{M}) = 2\sum_{k=-N+1}^{N-1} f(n+k)\cdot f^*(n-k)\cdot e^{-jkm(2\pi/M)}\cdot w(k)\cdot w^*(-k) \quad , \qquad (2)$$

where

k : is the dummy-variable representing the time domain,
2N-2 : is the length of the window,
M : is the number of points in the DFT (i.e. 2N-2),
n,m : are the discrete time and frequency index, respectively,
f : is the discrete-time input complex signal, and
f^* : is the complex conjugate of the input signal.

The Wigner-Ville method will be tested with discrete-time input signals. In order to speed up the computation, the FFT technique will be used for the evaluation of this distribution.

The flowcharts of the algorithms developed for the evaluation of this distribution are given in Figure 3 for non-analytic signals, and in Figure 4 for analytic signals. As with the CWD, the input to the WVD must be analytic.

For a more detailed discussion of the theory behind the Wigner-Ville distribution and its properties, the interested reader can refer to the papers by Claasen and Mecklenbräuker [3]-[5], Andrieux, Feix, Mourgues, Bertrand, Izrar and Nguyen [6], Boashash and Black [7], Peyrin and Prost [8], Amin [9], and Cohen [1].

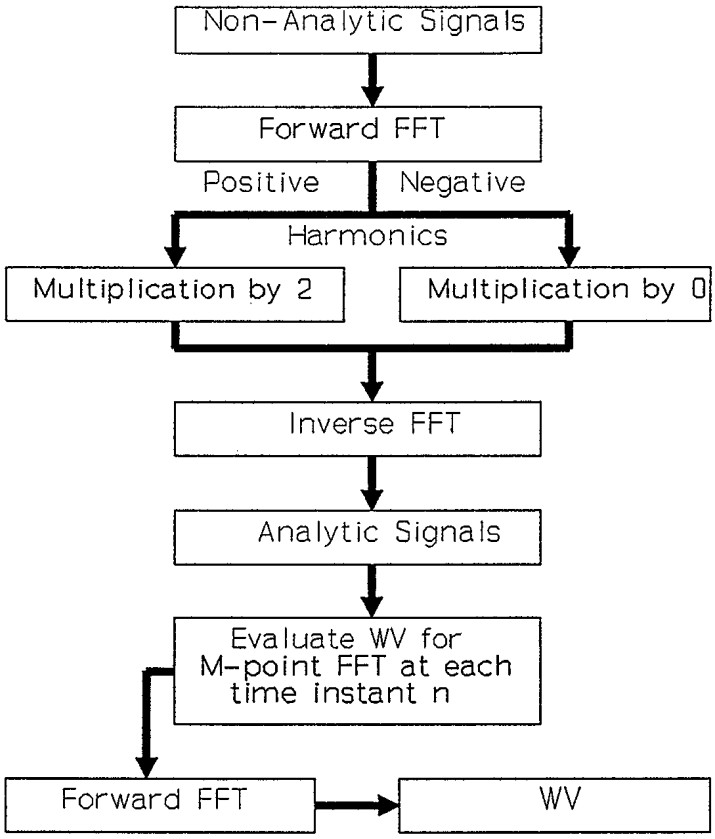

Figure 3. Flowchart of the algorithm used for the evaluation of the Wigner-Ville distribution with non-analytic input signals.

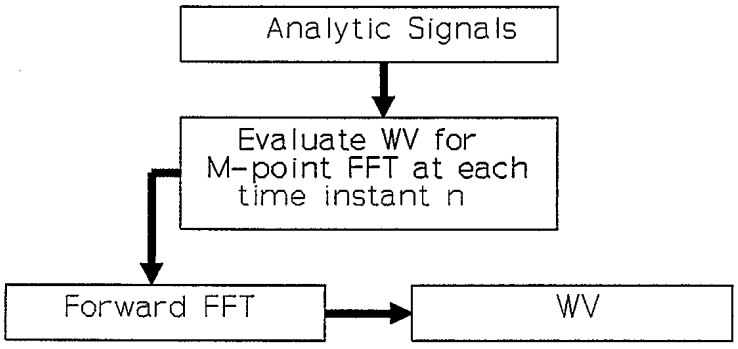

Figure 4. Same as Figure 3, but for analytic input signals.

3. TESTING THE TFDs AND DFT

3.1. Description of test data

Tests of the two time-frequency distribution techniques were conducted to determine their ability to resolve, in both time and frequency, various stationary and non-stationary discrete signals. The input signals used for testing include the following four types of data:

- One Sinusoidal signal (used to illustrate whether the frequency of the signal is estimated correctly) :

$$y(n) = \sin(2\pi\, fn/\text{sampling rate}), \tag{3}$$

- Two Sinusoidal signals (used to illustrate the effects on the cross-terms of each distribution for stationary signals) :

$$y(n) = \sin\left(\frac{2\pi f_1 n}{\textit{sampling rate}}\right) + \sin\left(\frac{2\pi f_2 n}{\textit{sampling rate}}\right) , \tag{4}$$

- Two Linear Frequency Modulation (LFM) signals (used to illustrate the effects on the cross-terms of each distribution for nonstationary signals) :

$$y(n) = 4.0\cos\left(2\pi(\frac{n}{8})(\frac{n}{256})\right) + 4.0\cos\left(2\pi(\frac{(512-n)}{8} + 40)(\frac{n}{256})\right) , \tag{5}$$

- Two records of real range-compressed temporal radar data, with 4096 complex data points per record, representing the radar backscatter through time of different scatterers (sampled at 575 samples per second), designated as:

  - REC336
  - REC358

This last data source was included to illustrate the effects on the signal resolvability and noise immunity of both distributions.

The first three types of signals were converted to analytic signals prior to being processed by the two TFD functions. As the radar data is already bandlimited to the range $-\pi/2$ to $\pi/2$, aliasing problems in the TFD functions are avoided for this last type of signal. Note that only the real test signals contain multiplicative and additive noise, while the other

signals are noise-free.

The signals described above were also analyzed with the DFT technique. The FFT was used for the computation. The results obtained with the DFT form a basis for comparison since this technique is the standard approach for the spectral analysis of discrete-time signals.

All output test results will be presented as plots of the magnitude, in dBs, of the output spectrum from each technique. These results will be given in the following sections.

3.2. Discrete Fourier Transform analysis of test data

Prior to testing the two distribution techniques, a baseline was determined by using the short-time DFT to compute the spectrum of each test signal at various time intervals. The extracted time intervals were passed through a Hamming window to reduce sidelobe levels. The window is defined as :

$$W(n) = 0.54 - 0.46\,COS\left(\frac{2\pi n}{N-1}\right), \quad 0 \le n \le N-1 .$$

The size of the DFT and window was 128 points. The DFT was implemented using the FFT technique. The magnitude of the spectral output from the FFT, for each signal described in Section 3.1, is plotted in Figures 5 to 14. The FFT routine given in reference [11] was used. The code for this routine can be found in Appendix A.1.

The first three signals tested were non-complex, hence, their spectral response in the positive frequency domain is identical to their response in the negative frequency domain. The real radar data is complex, and so this replication of the spectrum does not occur.

In Figure 6, F1 and F2 refer to the two frequencies in Equation (4).

In Figures 7 to 14, T refers to the time index of the signal (ranging from 1 to 4096) at the start of the block of data used for analysis. The signal-to-noise ratios for the spectra in each of Figures 9 to 14 have been computed and can be found in Table 4.

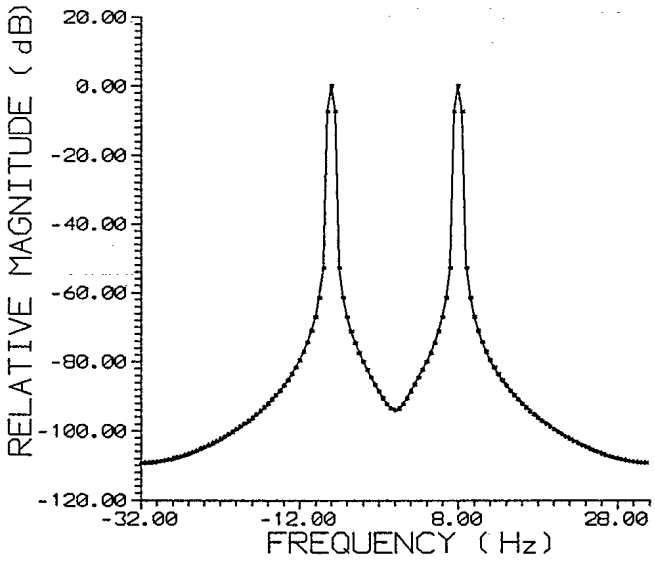

Figure 5. FFT of one sinusoidal signal with a Frequency of 8 Hz and a sampling rate of 64 samples per second.

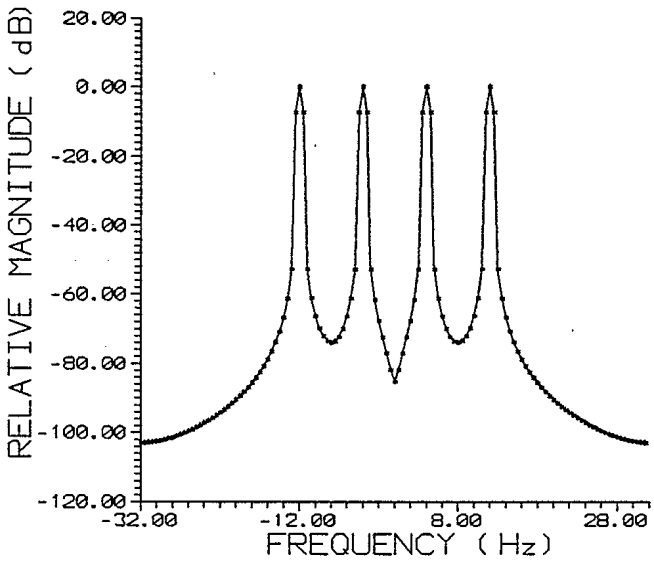

Figure 6. FFT of two sinusoidal signals with frequencies F1 = 4 Hz and F2 = 12 Hz, and a sampling rate = 64 samples per second.

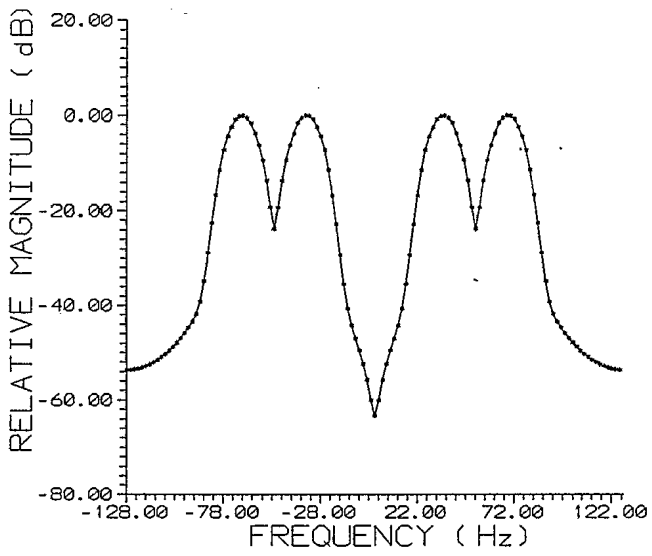

Figure 7. FFT of two LFM signals at T = 79.

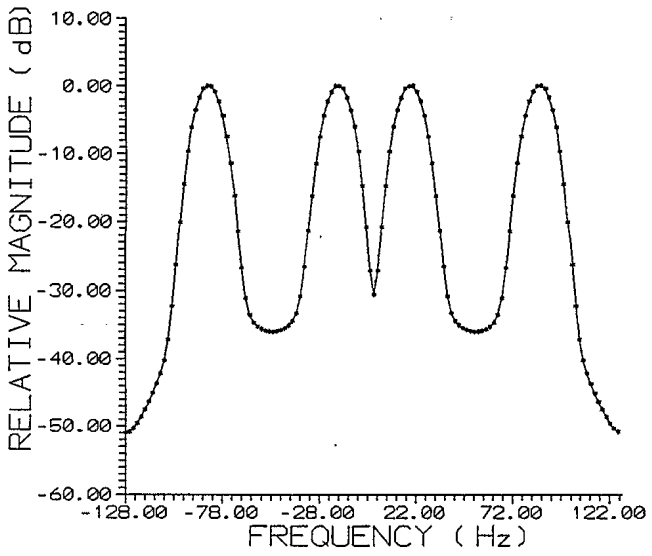

Figure 8. FFT of two LFM signals at T = 279.

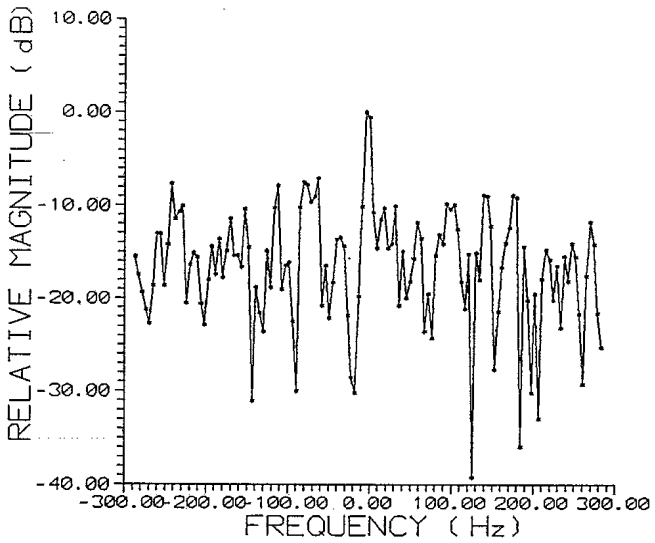

Figure 9. FFT of REC336 at T = 79.

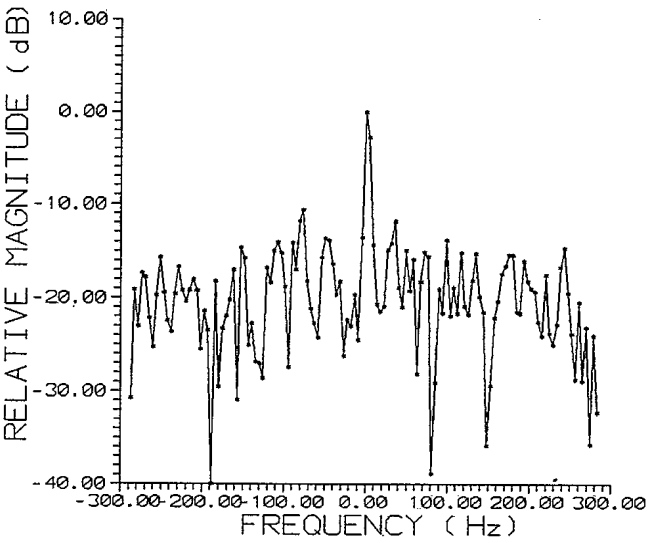

Figure 10. FFT of REC336 at T = 279.

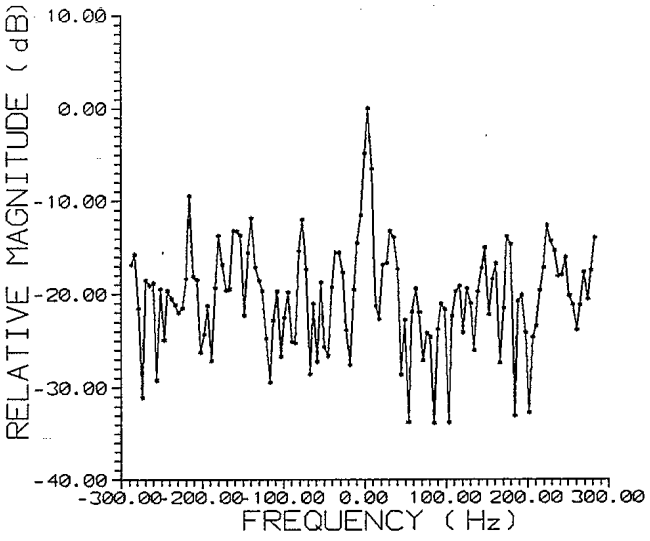

Figure 11. FFT of REC336 at T = 579.

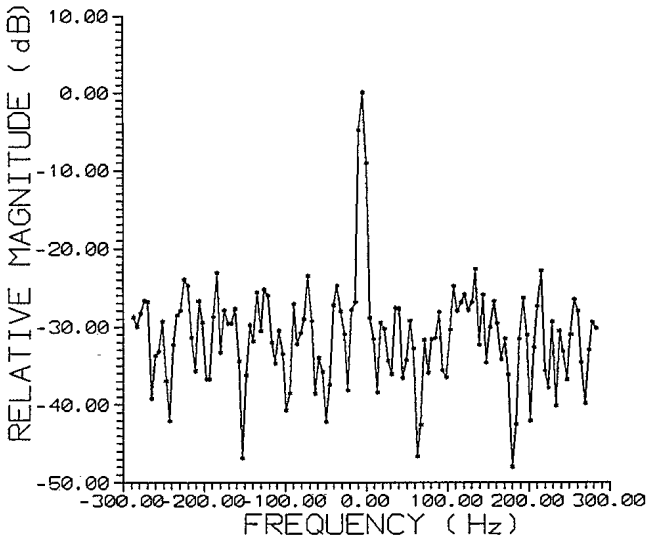

Figure 12. FFT of REC358 at T = 79.

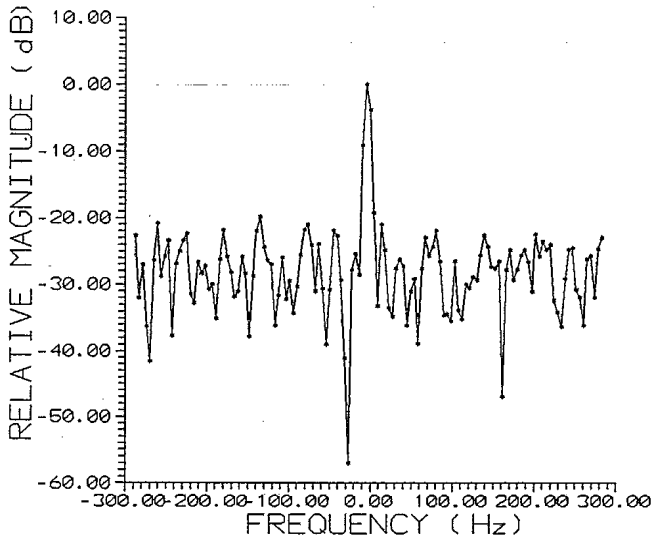

Figure 13. FFT of REC358 at T = 279.

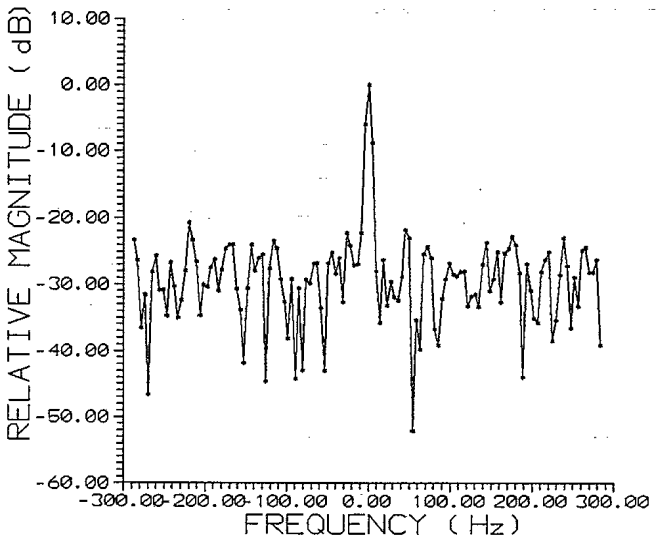

Figure 14. FFT of REC358 at T = 579.

3.3. Testing the Choi-Williams Distribution

This section presents the magnitude of the output spectral results from the Choi-Williams Distribution (CWD) for each of the input signals described in Section 3.1. The code used to implement the CWD can be found in Appendix A.2.

In this section, the windows of the CWD,

$$W_N(n)\ ,\ W_M(n)$$

are set to be rectangular windows with lengths N = 128 and M = 29. The selection of these values was based on suggestions given in reference [2]. Test results with a Hamming window can be found in Section 3.6.

While testing the CWD with various signals, it is possible to exercise control over the level of the cross-terms and the degree of resolvability of the signals by simply adjusting the amplitude scaling parameter, σ. A typical value for σ, as suggested in [2], is 1.0. For our own test signals, a value of σ = 3.0 is used. The reason for selecting this value is given in Section 3.5.1.

Figure 15 shows the CWD of the sinusoidal signal at T = 79. This figure can be compared to Figure 5, which is the FFT of the same signal. Although the resolvability of the signal at -30 dBs is similar for both techniques (i.e. approximately 2 Hz), the signal energy is more concentrated in Figure 5. This may be due to the fact that the signal is windowed prior to taking its FFT, but no window is applied prior to computing the CWD.

While testing with the two sinusoidal signals, different values of σ were used to illustrate how the ratio of the signal-to-cross-term signal level changes. The values σ = 0.1, 10.0, and 3.0, at a time T = 79, were used and the CWD results are plotted in Figures 16 to 18, respectively. For values of σ = 3.0 and 10.0, the resolvability of the two sinewaves is better with the CWD than with the FFT (see Figure 6). However, the signal energy is more concentrated in the FFTed signal. As with the single sinewave, the lack of any windowing in the CWD may be the cause of reduced signal energy concentration.

Figures 19 to 22 show the CWD of the two LFM signals, defined by Equation (5), for different values of T. As T increases, the two signals approach each other, then cross each other, and spread apart. It can be observed from this sequence of plots, that the resolvability of the signals, as well as the relative cross-term level, remain fairly constant. Thus, it appears that for non-stationary signals without noise, the CWD gives consistent results through time. Comparing these plots to the ones in Figures 7 and 8 (representing the FFT of the LFM signals), it can be readily seen that the signals are better resolved in the CWD, but that the cross-term levels are higher in the CWD.

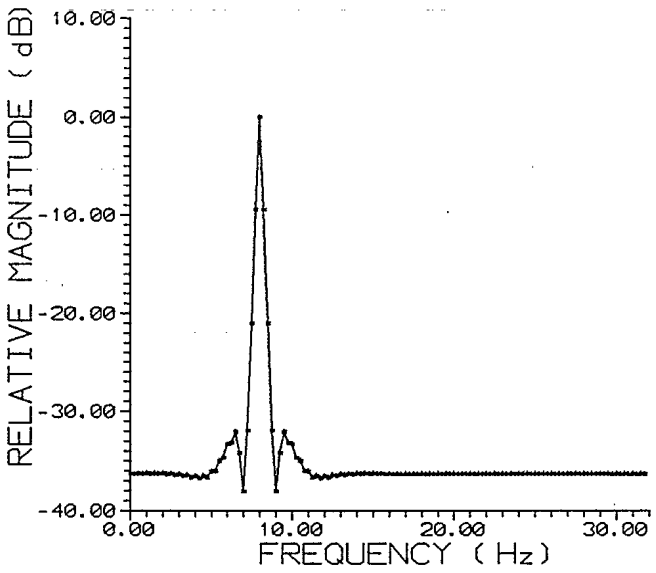

Figure 15. CWD of a sinusoidal signal at T = 79 with a frequency of 8 Hz, a sampling rate of 32 samples per second, and σ = 3.0.

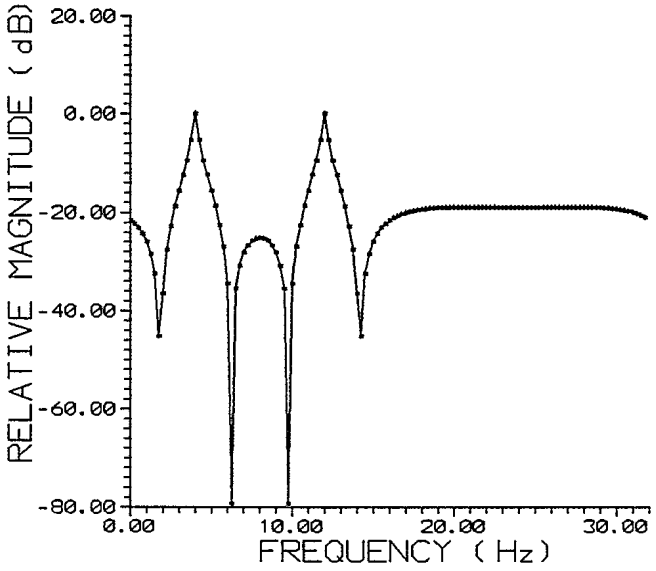

Figure 16. CWD of two sinusoidal signals at T = 79 with frequencies F1 = 4 Hz and F2 = 12 Hz, at a sampling rate of 32 samples per second, and σ = 0.1.

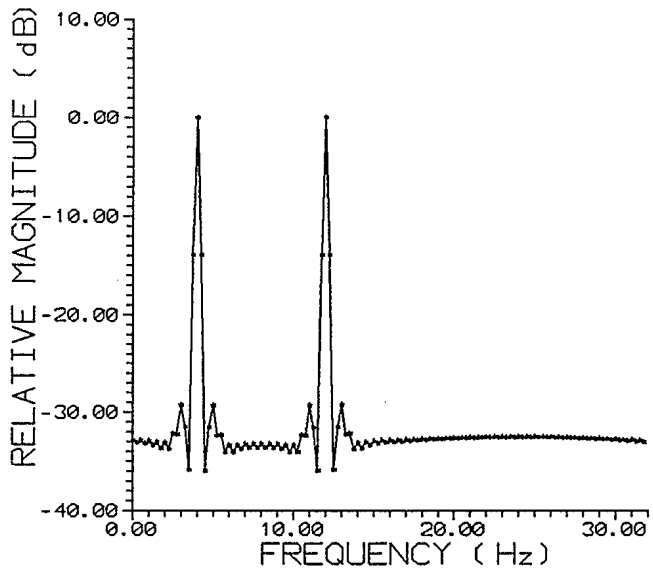

Figure 17. CWD of two sinusoidal signals at T = 79 with frequencies F1 = 4 Hz and F2 = 12 Hz, at a sampling rate of 32 samples per second, and σ = 10.0.

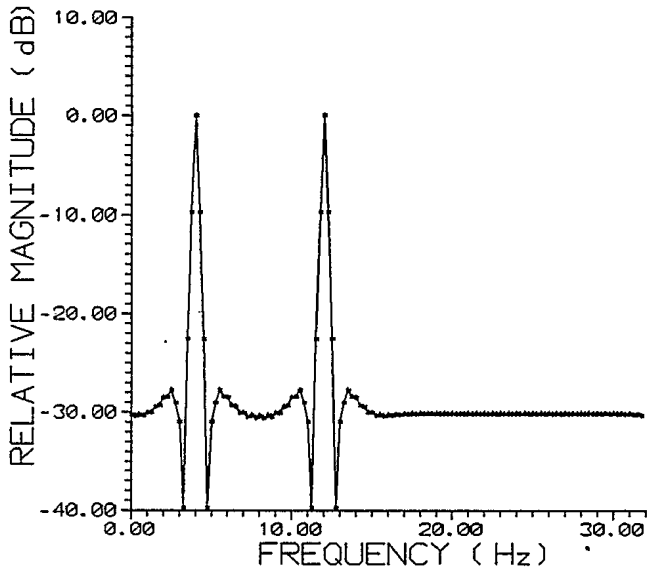

Figure 18. CWD of two sinusoidal signals at T = 79 with frequencies F1 = 4 Hz and F2 = 12 Hz, at a sampling rate of 32 samples per second, and σ = 3.0.

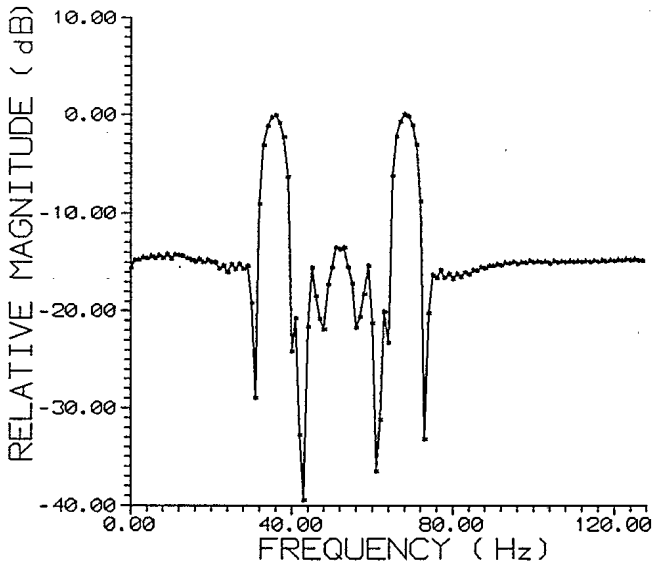

Figure 19. CWD of two LFM signals at T = 79 and σ = 3.0.

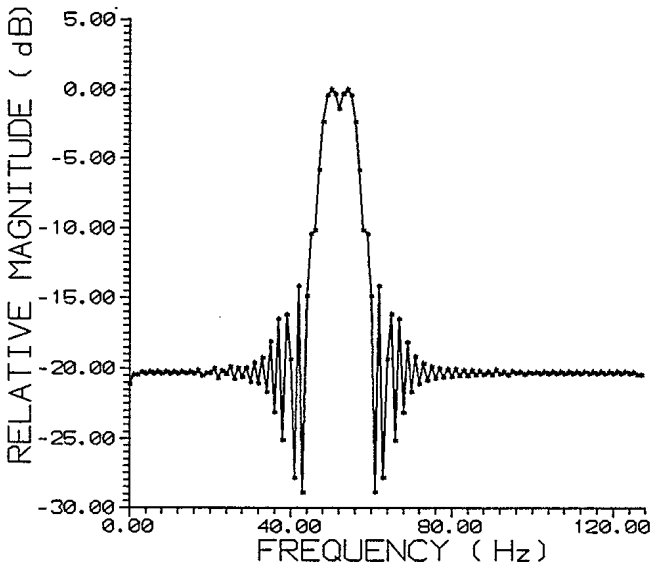

Figure 20. CWD of two LFM signals at T = 129 and σ = 3.0.

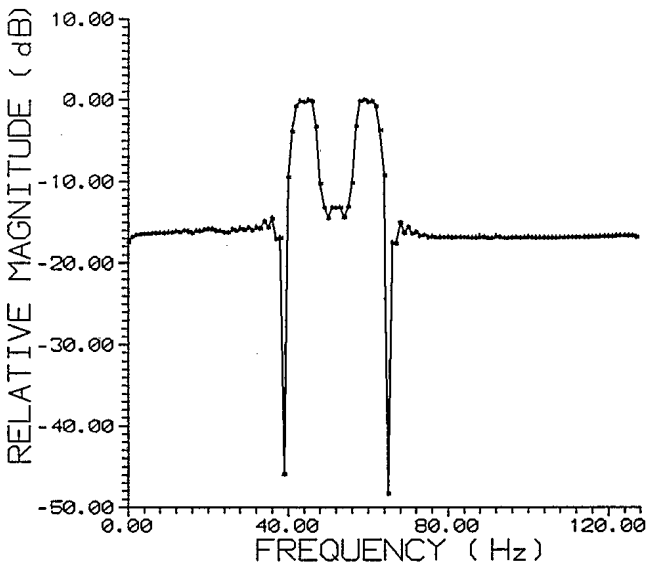

Figure 21. CWD of two LFM signals at T = 179 and σ = 3.0.

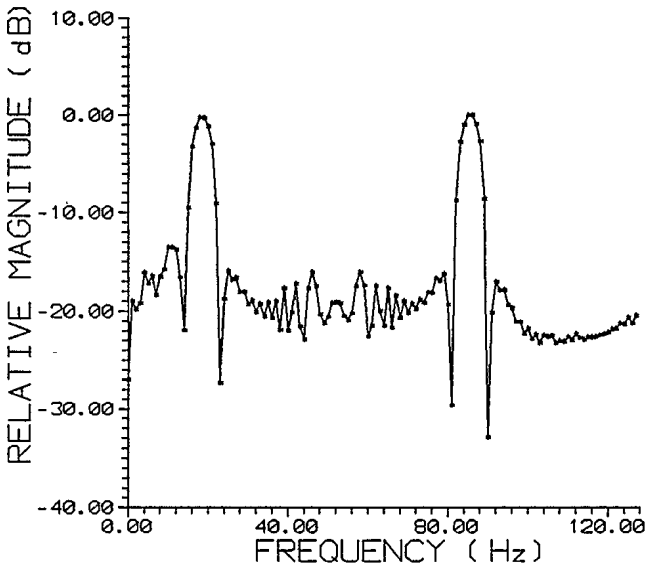

Figure 22. CWD of two LFM signals at T = 279 and σ = 3.0.

Figures 23 to 28 show the CWD of the two records of real radar data for different values of T. This sequence of six plots may be compared to those in Figures 9 to 14, respectively. A comparison of their SNRs is given in Section 3.5.2. It can generally be observed that the CWD is better able to resolve the radar signal than the FFT (i.e. about 8 Hz for the CWD versus about 15 Hz for the FFT), and that the SNR is higher for the CWD.

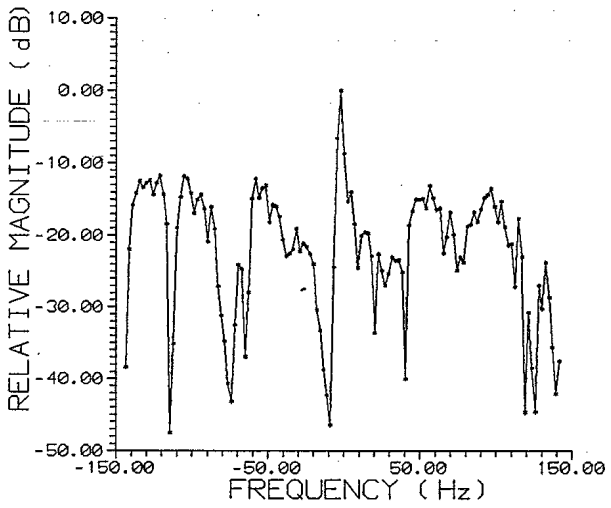

Figure 23. CWD of REC336 at T = 79 and σ = 3.0.

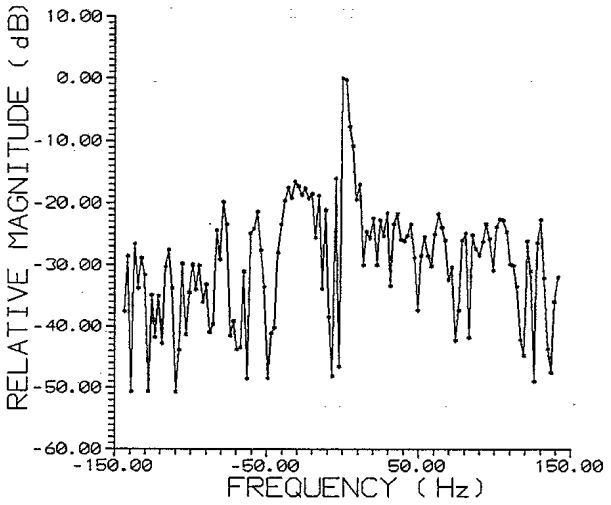

Figure 24. CWD of REC336 at T = 279 and σ = 3.0.

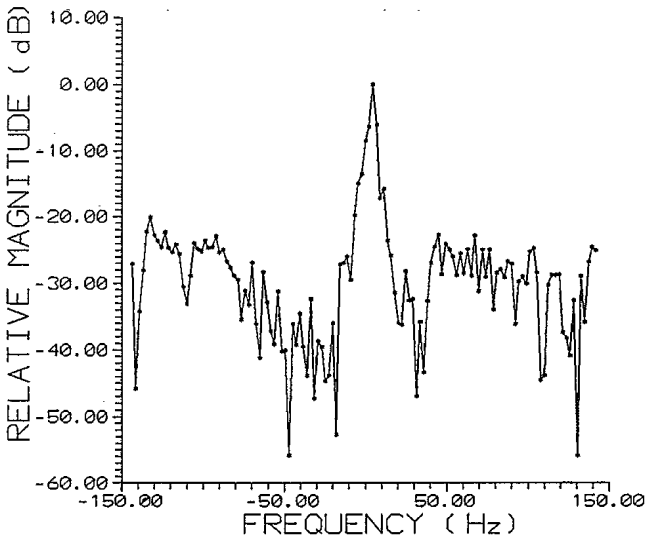

Figure 25. CWD of REC336 at T = 579 and σ = 3.0.

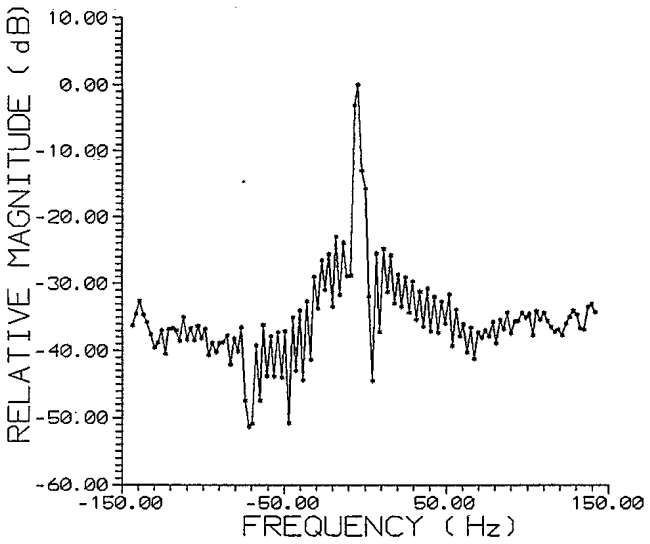

Figure 26. CWD of REC358 at T = 79 and σ = 3.0.

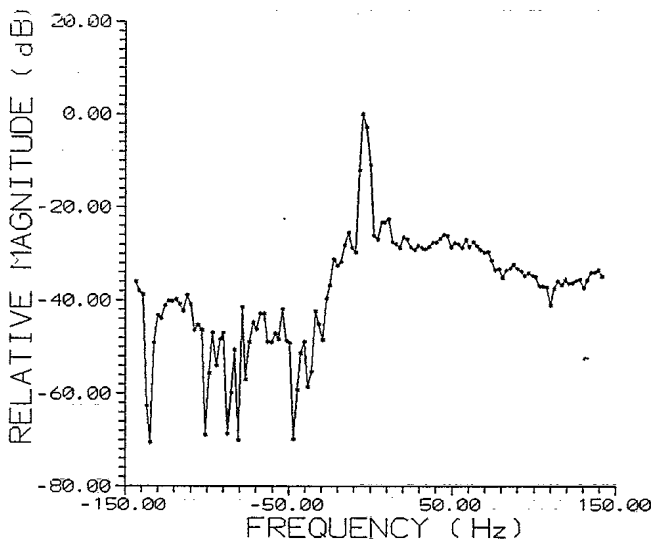

Figure 27. CWD of REC358 at T = 279 and σ = 3.0.

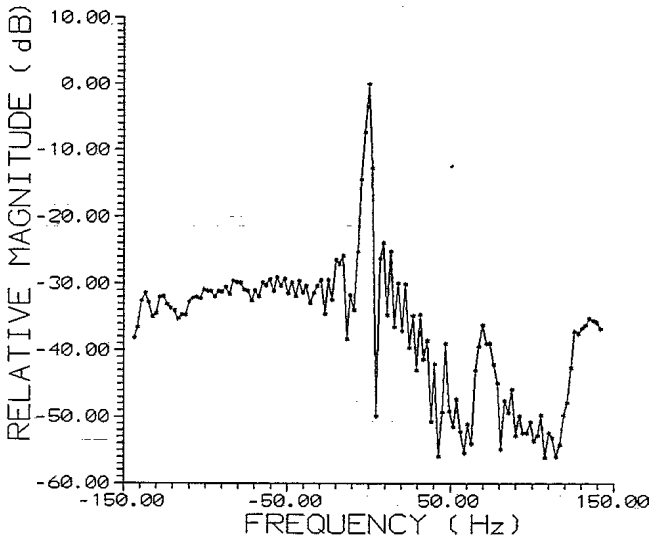

Figure 28. CWD of REC358 at T = 579 and σ = 3.0.

3.4. Testing the Wigner-Ville Distribution

In this section, the magnitude of the output spectrum from the Wigner-Ville Distribution (WVD) is presented for each of the input signals described in Section 3.1. With the WVD, no σ parameter is required. The code used to implement the WVD can be found in Appendix A.3.

From Equation (2), it can be seen that implementation of the WVD makes provision for the use of a window. The window used for testing was rectangular with a length N = 128. This is the same window as that used with the CWD.

Figure 29 shows the WVD of the sinusoidal signal at T = 79. This figure can be compared to Figures 5 (FFT results) and 15 (CWD results). Obviously, the WVD is able to better resolve this signal. It also concentrates the signal energy more than either the FFT or CWD. Hence, the WVD is able to perform far better on stationary monotone signals.

Figure 30 shows the WVD of the two sinusoidal signals at T = 79. This figure can be compared to Figures 6 (FFT results) and 18 (CWD results). Again, the WVD is able to better resolve both signals and to concentrate their energy more than either the FFT or CWD. In addition, the relative level of the cross-terms is negligible. Hence, the WVD is able to perform far better on stationary multi-component signals.

Figures 31 to 34 show the WVD of the two LFM signals for different values of T. The results in these figures can be compared to the results in Figures 7, 8 (FFT results), and 19 to 22 (CWD results). Although the two LFM signals are better resolved in the WVD (using the -3 dB point as a reference), definitely the relative level of the cross-terms are much higher than either the FFT or CWD (i.e. about -10 dB for the WVD versus about -20 dB for the CWD). Hence, the WVD does not perform as well with non-stationary multi-component signals.

Figures 35 to 40 show the WVD of the two records of real data for different values of T. A general comparison of these figures to Figures 9 to 11 (FFT results for REC336) and 23 to 25 (CWD results for REC336) shows that the WVD has a difficult time resolving REC336. Section 3.5.2 will compare the SNR of all these figures. Then, it will be seen that the SNR of the WVD is the worst of all three techniques. Hence, the WVD does not perform as well with non-stationary noisy signals. Since these signals represent real world signals, the WVD would not be an ideal choice to perform spectral analysis for this type of signal.

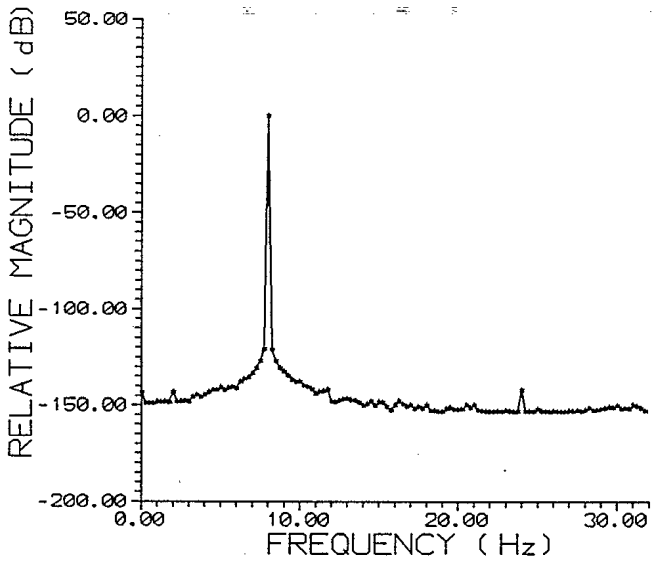

Figure 29. WVD of a sinusoidal signal at T = 79, with a frequency of 8 Hz and a sampling rate of 32 samples per second.

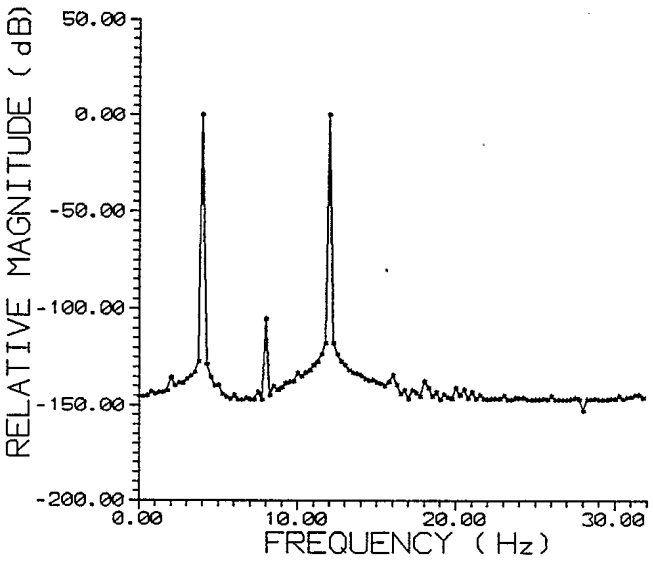

Figure 30. WVD of two sinusoidal signals at T = 79, with frequencies F1 = 4 Hz and F2 = 12 Hz, and a sampling rate of 32 samples per second.

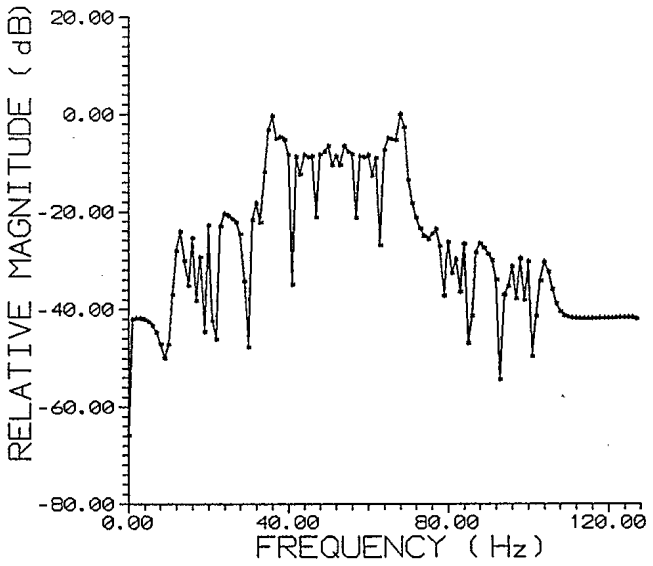

Figure 31. WVD of two LFM signals at T = 79.

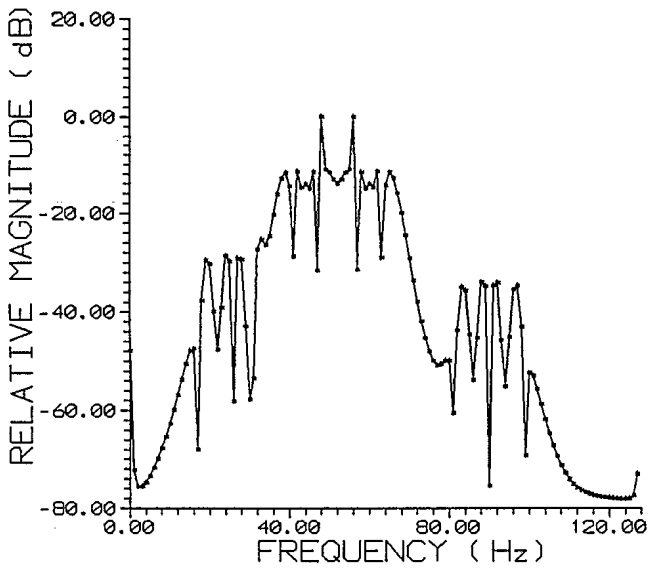

Figure 32. WVD of two LFM signals at T = 129.

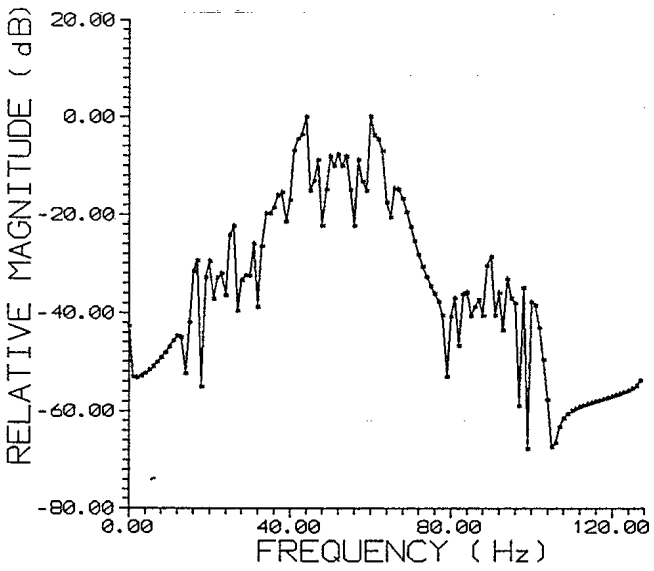

Figure 33. WVD of two LFM signals at T = 179.

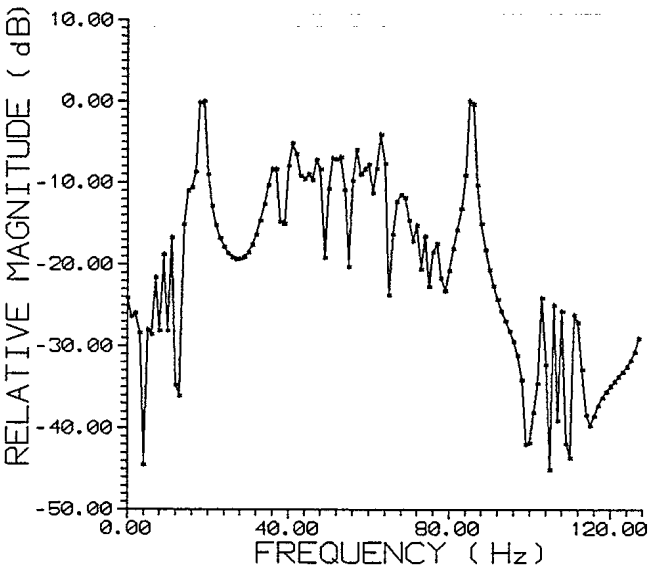

Figure 34. WVD of two LFM signals at T = 279.

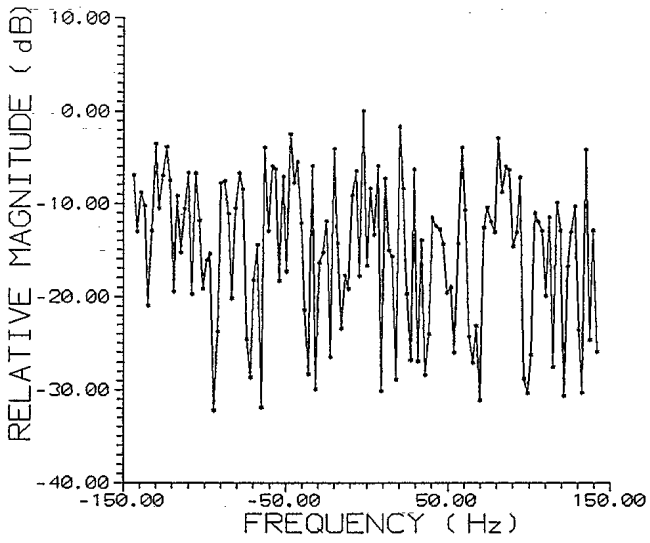

Figure 35. WVD of REC336 at T = 79.

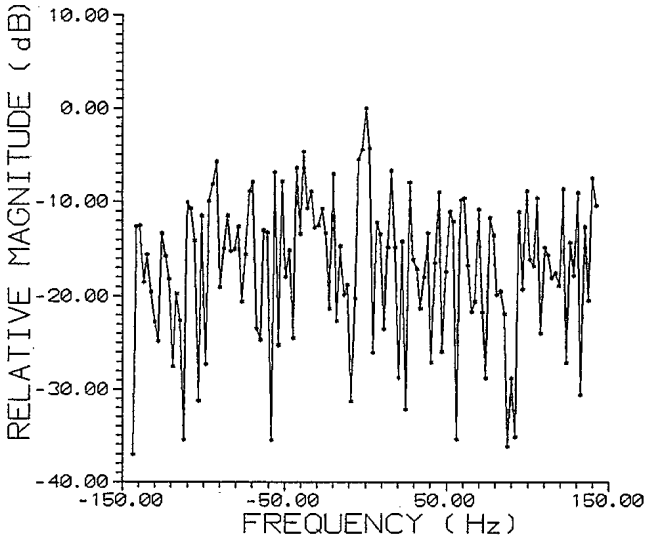

Figure 36. WVD of REC336 at T = 279.

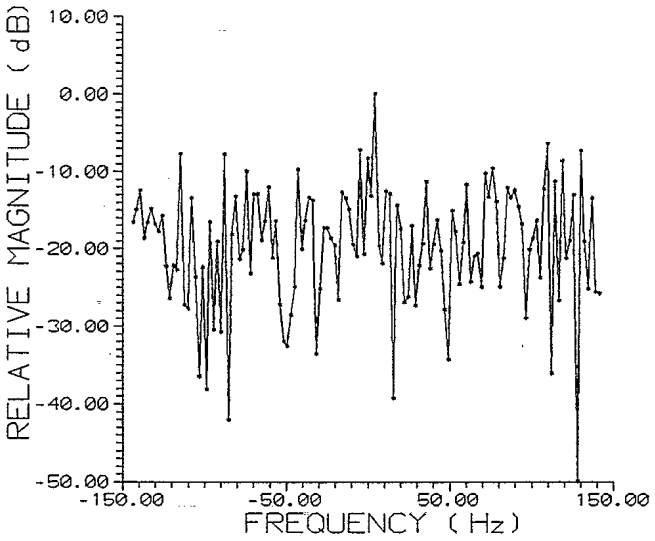

Figure 37. WVD of REC336 at T = 579.

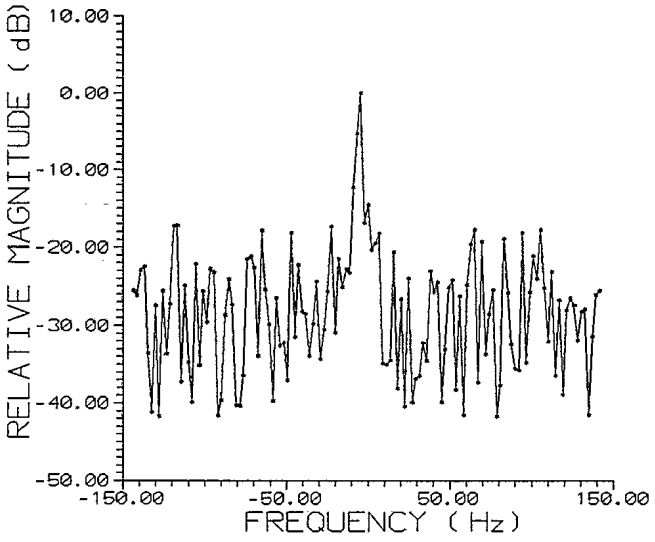

Figure 38. WVD of REC358 at T = 79.

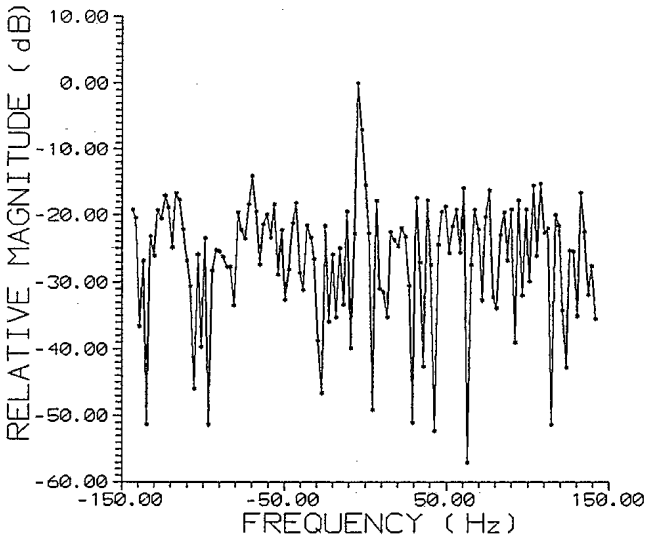

Figure 39. WVD of REC358 at T = 279.

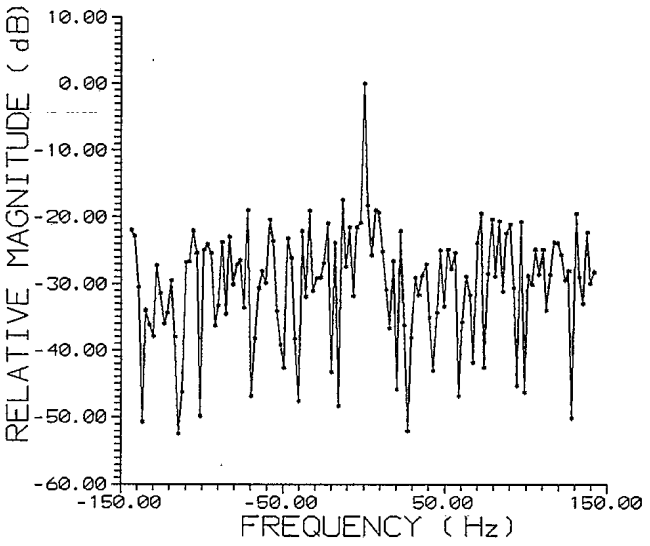

Figure 40. WVD of REC358 at T = 579.

3.5. Comparison of Test Results

In this section, a comparison of the relative levels of the cross-terms between the two distributions is made in order to determine which of the two distributions gives the highest signal-to-cross-term ratio. With the CWD, this ratio is maximized via the selection of a near optimum value for σ. In addition, a comparison of the SNR of each of the real radar signals is given for each distribution, including the DFT.

3.5.1. Comparison of the signal-to-cross-term ratio height

The signal-to-cross-term ratio height is defined as follows:

Ratio Height = (Maximum 1 / Maximum 2) , where

Maximum 1 : is the highest amplitude value of the true signal(s), and
Maximum 2 : is the highest amplitude of the cross-terms.

Since the cross-terms represent an unwanted composite signal or interference, similar to noise, the signal-to-cross-term ratio should be as high as possible.

Tables 1 and 2 provide examples of ratio heights for the CWD, for different signals and values of σ. These ratios are used to determine a near optimum value for σ. Adjusting σ causes the cross-term levels and signal resolvability to change. From Table 1 it can be observed that the largest ratio height occurs at σ = 5.0, while the largest ratio height in Table 2 occurs at σ = 1.0. Hence, the value of σ which maximizes the ratio height appears to be dependent on the signal. For testing the CWD in this study, an average value of σ = 3.0 (i.e. (1.0 + 5.0)/2) was selected as representing an approximate optimum value.

Table 1. Ratio heights of two sinusoidal signals for CWD, with N = 128, M = 29, F1 = 4.0 Hz, F2 = 12.0 Hz and a sampling rate = 32.0 samples per second.

T	σ	Ratio Height
79	0.1	18.0250
79	1.0	19.4640
79	2.0	22.9884
79	3.0	24.3925
79	4.0	26.1146
79	5.0	26.8160
79	6.0	26.2445

Table 2. Ratio heights of two LFM signals for CWD, with N = 128 and M = 29.

T	σ	Ratio Height
79	0.1	6.5920
79	1.0	14.3664
79	2.0	6.6651
79	3.0	4.7358
79	4.0	3.9374
79	5.0	3.4689
79	6.0	3.1524

Having maximized the signal-to-cross-term ratio for the CWD of the signals being tested, a comparison of ratio heights between both distributions can be made. Table 3 presents the ratio heights for the CWD and WVD. A comparison of the results shows that the CWD is consistently better than the WVD. In other words, the true signals are more easily detected in the CWD than in the WVD. However, comparing the plots in Figures 18 to 22 directly to the plots in Figures 30 to 34, it can be seen that the signals are better resolved in frequency, at the -3 dB point, in the WVD. Hence, the choice of using either a CWD or a WVD for spectral analysis of these types of signals depends upon the application. To detect signals, the CWD should be used, but to determine the exact frequency of a signal, the WVD should be used.

3.5.2. Comparison of the signal-to-noise ratio (SNR) for the two real signals

Of all the data used for testing, only the two real radar signals contained noise. Thus, based on this data, a comparison of the signal-to-average noise ratios (SNRs) is made of the output spectral data from both distribution techniques and the DFT. To compute the SNR, the location of the signal was first derived using the location of the maximum valued frequency bin, and then the energy in all other frequency bins which excluded the signal (assumed to be three frequency bins wide) were averaged to determine the mean noise value. This value was divided into the peak signal level to derive a measure of the SNR. The SNRs (in dBs) of the two distributions and the DFT for the two real radar signals are given in Table 4. It can be seen that the CWD gives the highest SNR in all cases, while the WVD gives the lowest SNR in all cases. However, the resolvability of the signals is similar for both distributions, and higher than that of the DFT. It would appear that for this type of signal, the CWD would be best to use to perform a spectral analysis.

Table 3. Ratio heights of two LFM signals for both TFDs, with N = 128 and M = 29.

T	σ	Choi-Williams	Wigner-Ville
		Ratio Height	Ratio Height
1	3.0	6.2196	1.3355
51	3.0	6.0465	2.9974
61	3.0	2.5321	2.0343
201	3.0	2.5321	2.0343
301	3.0	6.3534	1.7173
501	3.0	5.5184	1.7414
801	3.0	6.0720	1.4668

Table 4. SNR of the two real radar signals for the DFT, CWD and WVD at different T.

T	DFT		CWD		WVD	
	REC336	REC358	REC336	REC358	REC336	REC358
79	14.34	26.89	18.22	29.14	11.65	23.94
279	18.21	24.57	23.65	28.45	13.81	22.20
579	18.06	25.58	24.56	29.47	16.41	25.45

3.6. The CWD and WVD with a Hamming Window

In all tests described so far, the rectangular window was used with the TFDs. In an attempt to increase the SNR of the real radar signals, the Hamming window was also studied for both TFDs. The SNRs obtained with the Hamming window are given in Table 5 for the CWD and Table 6 for the WVD.

Two cases were tested for the CWD. In one case, both windows were Hamming. In the second case, only the larger window was a Hamming window while the smaller window was a rectangular window.

A comparison of these results with those in Table 4 clearly indicates that both TFDs perform better without any windowing (i.e. a rectangular window). Furthermore, it is computationally simpler to use a rectangular window.

Table 5. SNR of the two real radar signals for the CWD with a Hamming window.

T	W_N and W_M are Hamming		W_N is Hamming and W_M is Rectangular	
	REC336	REC358	REC336	REC358
79	15.95	27.01	15.66	26.90
279	23.22	25.95	22.46	26.26
579	23.06	26.47	22.59	26.50

Table 6. SNR of the two real radar signals for the WVD with a Hamming window.

T	REC336	REC358
79	9.60	23.66
279	13.06	21.06
579	13.75	22.48

3.7. Varying the window size in the CWD

This section analyzes the effects of modifying the size of the two windows (i.e. N and M) on the CWD. The SNRs for the two real radar signals were obtained for various combinations of the values N and M. The results are given in Table 7.

The following general observations can be made from the results in Table 7. For a fixed value of M, the SNR increases with increasing value of N. The same is true for a fixed value of N and increasing value of M. This is simply a result of the fact that more of the signal, which is more coherent than the background noise, is used to compute its distribution. The number of samples of the signal which are used to compute the distribution is equal to NM, and it can be generally stated that the higher the NM value, the higher the SNR.

Comparing the SNRs in this table to the ones in Table 4 for the DFT, we may be able to conclude that as the value of M tends to 0, the CWD tends towards the DFT. However, this may not be universally true since the kernel of each function is different (i.e. $f(\tau)$ for the DFT versus $f(n+\tau)f^*(n-\tau)$ for the CWD).

Table 7. SNR of the two real radar signals for the CWD with different values of M and N.

T	M	N	REC336	REC358
79	29	64	12.72	26.69
79	20	128	16.34	27.87
79	29	128	18.22	29.14
79	29	256	20.61	31.11
79	64	128	21.72	31.08
279	29	64	21.13	26.04
279	20	128	22.40	27.41
279	29	128	23.65	28.45
279	29	256	26.02	30.88
279	64	128	26.07	31.04
579	29	64	22.47	26.29
579	20	128	23.34	27.91
579	29	128	24.56	29.47
579	29	256	25.80	30.61
579	64	128	27.13	31.89

4. CONCLUDING REMARKS

This paper described and tested two time-frequency distributions: the Choi-Williams and Wigner-Ville distributions. Many tests were conducted to illustrate how each technique could resolve stationary and nonstationary signals in both time and frequency. The results were compared to those obtained with the short-time DFT, which is the most standard method used for spectral analysis.

From the results presented, it is concluded that the CWD performs better than both the WVD and DFT. In particular, measures of the SNR for the real radar signals were highest for the CWD. Also, the signal-to-cross-term ratios for the CWD were higher than those obtained for the WVD.

Furthermore, for the sample lengths chosen, it was shown that a rectangular window performs better than a Hamming window when used in the CWD. In addition to the improved performance, the use of the rectangular window reduces the number of computations required. It was also observed that the SNR scales with sample length for the CWD. This is to be expected for a coherent signal buried in noncoherent noise. It is felt that to further support these two findings, additional tests should be performed with other types of nonstationary signals buried in noise. These signals can be simulated or real.

For the data considered, it was shown that a value of $\sigma = 3.0$ seemed to maximize the signal-to-cross-term ratio. However, no tests were performed to indicate how σ affects the SNR of the spectrum of the distribution. Such tests would be worthwhile since a more optimum value for σ may be found. Indeed, the optimum value of σ may be data dependent.

The results presented in this paper suggest that the CWD technique is superior to both the WVD and DFT techniques for the analysis of noisy nonstationary signals. Since these types of signals represent an important class of real signals, the CWD should be seriously considered as a replacement technique for the standard short-time DFT technique. The only apparent hinderance to using the CWD instead of the DFT is the increased number of computations required to implement the CWD. From Equation (1), we see that the extra computations come from computing the time indexed autocorrelation function. There would be roughly 16xNxM additional operations (this assumes that the window is rectangular and that the signal is complex). Therefore, it would take about $((16xNxM + N\log_2 N)/N\log_2 N)$ times longer to compute the CWD versus computing the FFT. This simplifies to $(16xM/\log_2 N + 1)$. For typical values of $M=20$ and $N=128$, it would take about 47 times more computations to compute the CWD versus the FFT.

5. APPENDIX A : List of Programs

A.1 Subroutine to compute FFT

```
*****  This subroutine is a realization of the Fast Fourier Transform theory

*****  Subroutine for calculating FFT
*      Taken from page 394 of Numerical Recipes.

      SUBROUTINE FFT(DATA,NN,ISIGN)
$DEBUG

      REAL*8 WR,WI,WPR,WPI,WTEMP,THETA,DATA[HUGE]
      DIMENSION DATA(2*NN)


      N=2*NN

      J=1
      DO 11 I=1,N,2
       IF(J.GT.I) THEN
         TEMPR=DATA(J)
         TEMPI=DATA(J+1)
         DATA(J)=DATA(I)
         DATA(J+1)=DATA(I+1)
         DATA(I)=TEMPR
         DATA(I+1)=TEMPI
       ENDIF
       M=N/2
1      IF ((M.GE.2).AND.(J.GT.M)) THEN
         J=J-M
         M=M/2
         GOTO 1
       ENDIF
       J=J+M
11     CONTINUE

      MMAX=2
2     IF (N.GT.MMAX) THEN
       ISTEP=2*MMAX
       THETA=6.28318530717959D0/(ISIGN*MMAX)
       WPR=-2.D0*DSIN(0.5D0*THETA)**2
```

```
      WPI=DSIN(THETA)
      WR=1.D0
      WI=0.D0

      DO 13 M=1,MMAX,2
        DO 12 I=M,N,ISTEP
          J=I+MMAX
          TEMPR=SNGL(WR)*DATA(J)-SNGL(WI)*DATA(J+1)
          TEMPI=SNGL(WR)*DATA(J+1)+SNGL(WI)*DATA(J)
          DATA(J)=DATA(I)-TEMPR
          DATA(J+1)=DATA(I+1)-TEMPI
          DATA(I)=DATA(I)+TEMPR
          DATA(I+1)=DATA(I+1)+TEMPI
12      CONTINUE
        WTEMP=WR
        WR=WR*WPR-WI*WPI+WR
        WI=WI*WPR+WTEMP*WPI+WI
13    CONTINUE
      MMAX=ISTEP
      GOTO 2
    ENDIF

*     Normalize inverse transform

    IF(ISIGN.EQ.-1) THEN
      DO 30 I=1,N
        DATA(I)=DATA(I)/FLOAT(NN)
30    CONTINUE
    ENDIF

*   Error found in published version. Description in book of wraparound
*   order is reversed.  The following lines rearrang the data to
*   conform to the storage format outlined in Numerical Recipes.

      DO 40 I=1,NN/2
       TEMPR=DATA(2*I-1)
       TEMPI=DATA(2*I)
       DATA(2*I-1)=DATA(N-(2*I-1))
       DATA(2*I)=DATA(N-2*I+2)
       DATA(N-(2*I-1))=TEMPR
       DATA(N-2*I+2)=TEMPI
40    CONTINUE

*   Shift everything up two array subscripts
```

```
      TEMPR=DATA(N-1)
      TEMPI=DATA(N)
      DO 50 I=NN,2,-1
        DATA(2*I-1)=DATA(2*I-3)
        DATA(2*I)=DATA(2*I-2)
50     CONTINUE
      DATA(1)=TEMPR
      DATA(2)=TEMPI

      RETURN
      END
```

A.2 Subroutine to compute CWD.

```
*       ----------////////////----------
*
*       Subroutine for evaluating the Choi-Williams
*       distribution for a discrete time signal.
*
*       S( ) - (Signal) Real and imaginary parts of the signal
*       alternate
*       CWD( ) - (Distribution)
*       FS( ) - Array for storing FFT of S
*       ITNUM - Iteration Number
*       ACFN( ) - Time indexed auto-correlation function
*       SIGMA - Parameter of Choi-Williams Distribution
*            N,M - size of rectangular windows
*            Bigt - Number of points in input data file (Note: Power of 2)
*            Magcwd - matrix of calculated magnitude of complex numbers of CWD
*
*       ----------////////////////////----------

      SUBROUTINE CW(S,M,N,SIGMA,CWD,BIGT,MAGCWD)

      REAL*8 A1,A,B,C,D,F[HUGE],REFF,IMFF,P2,P3
      REAL*8 ACFN[HUGE],WN[HUGE],WM[HUGE],SIGMA,TAU,MU
      REAL*8 S[HUGE],CWD[HUGE],MAGCWD[HUGE]
      DIMENSION F(2100),ACFN(2100),WN(2100),WM(2100),S(2100)
      DIMENSION CWD(2100),MAGCWD(1050)
      INTEGER ITNUM,BIGT,K,FNUM,INTERVAL,UNITNUM,T,KL1,P1
      PARAMETER (PI=3.1415926535)

*     Set up windowing arrays

      DO 10 I=1,2*N
        WN(I)=1.0
        ACFN(I)=0
10    CONTINUE
      DO 15 I=1,2*M
        WM(I)=1.0
15    CONTINUE

*     Obtain analytic signal from given real valued realization
*     S(t)
```

```
      DO 20 I=1,2*BIGT
        F(I)=S(I)
20    CONTINUE

      CALL FFT(F,BIGT,1)

*     Multiply positive harmonics by 2, and negative harmonics
*     by 0

      DO 30 I=1,BIGT
        F(I)=2*F(I)
30    CONTINUE
      DO 40 I=BIGT+3,2*BIGT
        F(I)=0
40    CONTINUE
      IF(F(BIGT+1).LT.0) THEN
        F(BIGT+1)=0
        F(BIGT+2)=0
      ENDIF

*     Perform inverse FFT on F to finally obtain analytic
*     signal

      write(6,*)'executing inverse ...'

      CALL FFT(F,BIGT,-1)

*     Determine limits for evaluation of equation 20, p.868,
*     Ref.6

      NMIN=1+(M/2+N/2)
      NMAX=BIGT-(M/2+N/2)

*     Evaluation equation
      WRITE(*,*)'ENTER KL1 '
         READ(*,*)KL1
         write(*,*)' Please waiting ... '

      DO 45 T=NMIN,NMAX

       if ( T .EQ. KL1)  THEN

        WRITE(6,100)' executing N :=    ',T
100     FORMAT('+',A25,I7)
```

```
      DO 50 TAU=-N/2,N/2
        IF (TAU.EQ.0) GOTO 50
        DO 60 MU=-M/2,M/2
          A1=4*TAU**2/SIGMA
          A2=2*(T+MU+TAU)-1
          A3=2*(T+MU-TAU)-1

          A=F(A2)
          B=F(A2+1)
          C=F(A3)
          D=F(A3+1)
          REFF=A*C+B*D
          IMFF=C*B-A*D
          ACFN(2*TAU+N+1)=ACFN(2*TAU+N+1)+((WM(MU+M/2+1)*1)/
     +      SQRT(A1*PI))*EXP(-1*MU**2/A1)*REFF
          ACFN(2*TAU+N+2)=ACFN(2*TAU+N+2)+((WM(MU+M/2+1)*1)/
     +      SQRT(A1*PI))*EXP(-1*MU**2/A1)*IMFF
60        CONTINUE
50      CONTINUE

      DO 70 TAU=1,2*N
        CWD(TAU)=2*WN(TAU)*ACFN(TAU)
70      CONTINUE

      CALL FFT(CWD,N,1)

*     Calculate magnitude for plotting and saving data in a file.

      OPEN(UNIT=4,FILE='CW.DAT',FORM='FORMATTED')

      DO 52 I=1,2*N-1,2
        P1=(I+1)/2
        P2=CWD(I)
        P3=CWD(I+1)
        MAGCWD(P1)=SQRT(P2*P2+P3*P3)
        WRITE(4,1992)P1,MAGCWD(P1)
1992      FORMAT(I8,E18.8)
52      CONTINUE

        CLOSE(UNIT=4,STATUS='KEEP')
      ENDIF
45  CONTINUE
    RETURN
    END
```

A.3 Subroutine to compute WVD.

```
**********************************************************************
*       Subroutine for determining the Wigner Ville
*       Distribution of a discrete signal in the time domain
**********************************************************************
******      S - Matrix of complex numbers of input data
******      WVD - Matrix of complex numbers of output data
******      Bigt - Number of points of input data

      SUBROUTINE WV(S,WVD,BIGT)

      REAL*8 S[HUGE],F[HUGE],WVD[HUGE],WVD2[HUGE],RECOEFF(0:20)
      REAL*8 MAGWV[HUGE],INT1(0:20),REINT2(0:20),MAGS[HUGE]
      REAL*8 PERROR(1050),PMAX,TEMP[HUGE],P2,P3
      REAL*8 A,B,C,D
      INTEGER A1,A2
      INTEGER BIGT,NMIN,NMAX,T,B1,B2,MAXNUM,N,UNITNUM,V,P1
      INTEGER OLDUNIT,SIGNAL,RECNUM,INTERVAL,I,K,index
      DIMENSION S(2100),WVD(2100),F(2100),MAGWV(2100)
      DIMENSION WVD2(2100),MAGS(2100),TEMP(2100)
      PARAMETER(PI=3.1415926535)


*       Do Hilbert Transform on discrete signal to get
*       analytical signal

      DO 20 I=1,2*BIGT
        F(I)=S(I)
20     CONTINUE
      CALL FFT(F,BIGT,1)

*       Multiply positive harmonics by 2, and negative
*       harmonics by 0

      DO 30 I=1,BIGT
        F(I)=2.0*F(I)
30     CONTINUE
      DO 40 I=BIGT+3,2*BIGT
        F(I)=0.00
40     CONTINUE
      IF(F(BIGT+1).LT.0) THEN
        F(BIGT+1)=0.00
```

```
        F(BIGT+2)=0.00
      ENDIF

*       Perform inverse FFT on F to finally obtain analytic
*       signal

      CALL FFT(F,BIGT,-1)

      DO 38 I=1,2*BIGT+1
        WVD(I)=0.00
38    CONTINUE

      WRITE(6,*)
      write(6,*)' enter index N '
      read(*,*)index

      NMIN = 1 + INDEX/2
      NMAX = BIGT - INDEX/2

      WRITE(6,*)'ENTER V '
      READ(*,*)V

*   evaluate equation

      DO 10 T = NMIN,NMAX
      IF (T .EQ. V) THEN
       DO 15 K=-INDEX/2,INDEX/2
         A1=2*(T+K)-1
         A2=2*(T-K)-1
           A=F(A1)
           B=F(A1+1)
           C=F(A2)
           D=F(A2+1)
           TEMP(2*K+INDEX+1)=(A*C+B*D)
           TEMP(2*K+INDEX+2)=(B*C-A*D)
15      CONTINUE

      WRITE(6,*)' WAITING PLEASE ... '

       DO 25 I=1,2*INDEX
         WVD(I)=2.0*TEMP(I)
25     CONTINUE

       CALL FFT(WVD,INDEX,1)
```

```
*    save data in file " wv.dat"

      OPEN(UNIT=4,FILE='WV.DAT',FORM='FORMATTED')

76       DO 52 I=1,2*INDEX-1,2
         P1=(I+1)/2
         P2=WVD(I)
         P3=WVD(I+1)
         MAGWV(P1)=SQRT(P2*P2+P3*P3)

         WRITE(4,1992)P1,MAGWV(P1)
1992      FORMAT(I8,E15.6)

52       CONTINUE

      CLOSE(UNIT=4,STATUS='KEEP')
      ENDIF

10    CONTINUE

      RETURN
      END
```

6. ACKNOWLEDGEMENTS

This work was supported by the Research and Development Branch of the Canadian Department of National Defence. Thanks also go to Dr. F. Tremblay for her review and editting of this paper.

7. REFERENCES

[1] L. Cohen, " Time-frequency distributions : A Review, " Proceedings of the IEEE, Vol. 37, NO. 7, pp. 941-981, 1989.

[2] H.I. Choi, W.J. Williams, " Improved time-frequency representation of multicomponent signals using exponential kernels, " IEEE Trans. Acoust., Speech, Signal Processing, Vol. ASSP-37, 1989.

[3] T.A.C.M. Claasen and W.F.G. Mecklenbrauker, " The aliasing problem in discrete-time Wigner Distributions, " IEEE Trans. Acoust., Speech, Signal Processing, Vol. ASSP-31, pp. 1067-1072, 1983.

[4] T.A.C.M. Claasen and W.F.G. Mecklenbrauker, " The Wigner distribution - a tool for time-frequency signal analysis; part I: continuous-time signals, " Philips J. Research, Vol. 35, pp. 217-250, 1980.

[5] T.A.C.M. Claasen and W.F.G. Mecklenbrauker, " The Wigner distribution - a tool for time-frequency signal analysis; part II: discrete-time signals, " Philips J. Research, Vol. 35, pp. 276-300, 1980.

[6] J.C. Andrieux, M.R. Feix, G. Mourgues, P. Bertrand, B. Izrar, and V.T. Nguyen, " Optimum smoothing of the Wigner-Ville distribution, " IEEE Trans. Acouts., Speech, Signal Processing, Vol. ASSP-35, pp. 764-769, 1987.

[7] B. Boashash and P.J. Black, " An efficient real-time implementation of the Wigner-Ville distribution, " IEEE Trans. Acoust., Speech, Signal Processing, Vol. ASSP-35, pp. 1611-1618, 1987.

[8] F. Peyrin and R. Prost, " A unified definition for the discrete-time, discrete-frequency, and discrete-time/frequency Wigner distributions, " IEEE Trans. Acoust., Speech, Signal Processing, Vol. ASSP-34, pp. 858-867, 1986.

[9] M.G. Amin, " Time and lag window selection in Wigner-Ville distribution, " Proceedings of the IEEE ICASSP 87, pp. 1529-1532, 1987.

[10] A.V. Oppenheim, R.W. Schafer, " Digital signal processing, " Prentice-Hall, Englewood Cliffs, 1975.

[11] W.H. Press, B.P. Flannery, S.A. Teukolsky, and W.T. Vetterling, " Numerical recipes - The art of scientific computing, " Cambridge University Press, 1986.

DOCUMENT CONTROL DATA

(Security classification of title, body of abstract and indexing annotation must be entered when the overall document is classified)

1. ORIGINATOR (the name and address of the organization preparing the document. Organizations for whom the document was prepared, e.g. Establishment sponsoring a contractor's report, or tasking agency, are entered in section 8.)

Defence Research Establishment Ottawa
3701 Carling Ave.
Ottawa, Ontario, K1A 0Z4

2. SECURITY CLASSIFICATION (overall security classification of the document. including special warning terms if applicable)

UNCLASSIFIED

3. TITLE (the complete document title as indicated on the title page. Its classification should be indicated by the appropriate abbreviation (S,C or U) in parentheses after the title.)

Testing Various Time-Frequency Distribution Techniques (U)

4. AUTHORS (Last name, first name, middle initial)

Robert D.J. Klepko and Khanh N. Tran

5. DATE OF PUBLICATION (month and year of publication of document)

October 1992

6a. NO. OF PAGES (total containing information. Include Annexes, Appendices, etc.)

51

6b. NO. OF REFS (total cited in document)

11

7. DESCRIPTIVE NOTES (the category of the document, e.g. technical report, technical note or memorandum. If appropriate, enter the type of report, e.g. interim, progress, summary, annual or final. Give the inclusive dates when a specific reporting period is covered.)

Technical Note

8. SPONSORING ACTIVITY (the name of the department project office or laboratory sponsoring the research and development. Include the address.)

Defence Research Establishment Ottawa
3701 Carling Ave.
Ottawa, Ontario, K1A 0Z4

9a. PROJECT OR GRANT NO. (if appropriate, the applicable research and development project or grant number under which the document was written. Please specify whether project or grant)

021LA

9b. CONTRACT NO. (if appropriate, the applicable number under which the document was written)

N/A

10a. ORIGINATOR'S DOCUMENT NUMBER (the official document number by which the document is identified by the originating activity. This number must be unique to this document.)

DREO TN 92-17

10b. OTHER DOCUMENT NOS. (Any other numbers which may be assigned this document either by the originator or by the sponsor)

11. DOCUMENT AVAILABILITY (any limitations on further dissemination of the document, other than those imposed by security classification)

(X) Unlimited distribution
( ) Distribution limited to defence departments and defence contractors; further distribution only as approved
( ) Distribution limited to defence departments and Canadian defence contractors; further distribution only as approved
( ) Distribution limited to government departments and agencies; further distribution only as approved
( ) Distribution limited to defence departments; further distribution only as approved
( ) Other (please specify):

12. DOCUMENT ANNOUNCEMENT (any limitation to the bibliographic announcement of this document. This will normally correspond to the Document Availabilty (11). However, where further distribution (beyond the audience specified in 11) is possible, a wider announcement audience may be selected.)

Full unlimited announcement.

UNCLASSIFIED

SECURITY CLASSIFICATION OF FORM

13. ABSTRACT (a brief and factual summary of the document. It may also appear elsewhere in the body of the document itself. It is highly desirable that the abstract of classified documents be unclassified. Each paragraph of the abstract shall begin with an indication of the security classification of the information in the paragraph (unless the document itself is unclassified) represented as (S), (C), or (U). It is not necessary to include here abstracts in both offical languages unless the text is bilingual).

(U) The representation of a signal in both the time and frequency domains is a major topic of study in the area of signal processing. Over the past 40 years, many plausible derivations and approaches of time-frequency distributions have been suggested. This paper tests two time-frequency distributions and compares their results. The two distributions are the discrete versions of the Wigner-Ville and Choi-Williams distributions. This paper will demonstrate the capability of each distribution to resolve discrete sinusoidal and real radar signals simultaneously in time and frequency. The radar data represents backscatter from a ship on the open ocean. The results will be compared to those obtained from the standard short-time Discrete Fourier Transform. (U)

14. KEYWORDS, DESCRIPTORS or IDENTIFIERS (technically meaningful terms or short phrases that characterize a document and could be helpful in cataloguing the document. They should be selected so that no security classification is required. Identifiers, such as equipment model designation, trade name, military project code name, geographic location may also be included. If possible keywords should be selected from a published thesaurus. e.g. Thesaurus of Engineering and Scientific Terms (TEST) and that thesaurus-identified. If it is not possible to select indexing terms which are Unclassified, the classification of each should be indicated as with the title.)

Time-Frequency Distributions
Wigner-Ville
Choi-Williams
Radar data
discrete signals
Discrete Fourier Transform

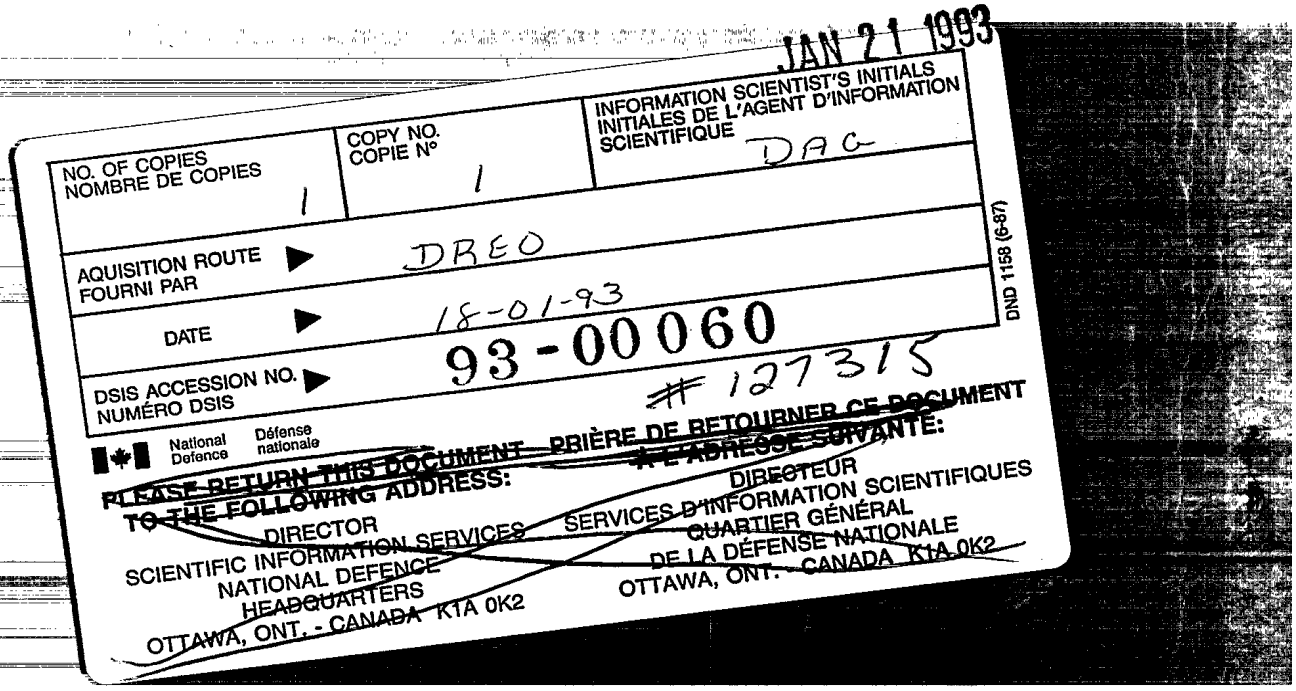

JAN 21 1993

NO. OF COPIES / NOMBRE DE COPIES	COPY NO. / COPIE N°	INFORMATION SCIENTIST'S INITIALS / INITIALES DE L'AGENT D'INFORMATION SCIENTIFIQUE
1	1	DAC

AQUISITION ROUTE / FOURNI PAR ▶ DREO

DATE ▶ 18-01-93

DSIS ACCESSION NO. / NUMÉRO DSIS ▶ 93-00060

#127315

DND 1158 (6-87)

National Defence / Défense nationale

~~PLEASE RETURN THIS DOCUMENT TO THE FOLLOWING ADDRESS:~~

DIRECTOR
SCIENTIFIC INFORMATION SERVICES
NATIONAL DEFENCE
HEADQUARTERS
OTTAWA, ONT. - CANADA K1A 0K2

~~PRIÈRE DE RETOURNER CE DOCUMENT À L'ADRESSE SUIVANTE:~~

DIRECTEUR
SERVICES D'INFORMATION SCIENTIFIQUES
QUARTIER GÉNÉRAL
DE LA DÉFENSE NATIONALE
OTTAWA, ONT. - CANADA K1A 0K2

CRAD / DRDIM 3
DEPARTMENT OF NATIONAL DEFENCE
OTTAWA ON K1A 0K2
CANADA